Bull. Chem. Soc. Ethiop. **2018**, 32(1), 111-124. ISSN 1011-3924
© 2018 Chemical Society of Ethiopia and The Authors Printed in Ethiopia
DOI: https://dx.doi.org/10.4314/bcse.v32i1.10

SYNTHESIS AND STRUCTURAL CHARACTERIZATION OF N-(2-{[(2E)-2-(2-HYDROXYBENZYLIDENE)HYDRAZINYL]CARBONYL}-PHENYL)BENZAMIDE (HL) AND ITS Co(II), Fe(III), Cu(II) AND Zn(II) COMPLEXES. X-RAY CRYSTAL STRUCTURE OF HL

Rasool Khan[1*], Aydin Tavman[2*], Demet Gürbüz[2], Mohammad Arfan[3] and Adem Çinarli[2]

[1]Institute of Chemical Sciences, University of Peshawar, Peshawar, 25120, Pakistan
[2]Istanbul University, Faculty of Engineering, Chemistry Department, Avcilar, 34320, Istanbul, Turkey
[3]H.E.J. Research Institute of Chemistry, International Center for Chemical and Biological Sciences (ICCBS) University of Karachi, Karachi, 75270, Pakistan

(Received November 11, 2017; Revised January 21, 2018; Accepted January 23, 2018)

ABSTRACT. *N*-(2-{[(2*E*)-2-(2-hydroxybenzylidene)hydrazinyl]carbonyl}phenyl)benzamide (**HL**) and its Co(II), Fe(III), Cu(II) and Zn(II) perchlorate complexes were synthesized. The structures of **HL** and its complexes were confirmed on the basis of elemental analysis and FT-IR, FT-Raman, ^{1}H-NMR spectra. TGA, magnetic moment and molar conductivity measurements were carried out for the complexes. In addition, the crystal structure of **HL** was determined by X-ray diffraction at room temperature. It crystallizes in the monoclinic, space group *C*2/c and *Z*=4. **HL** has an interesting structure due to the presence of two intramolecular hydrogen bonds. It behaves as a bidentate ligand through the C=N nitrogen and OH oxygen atoms in its chelate complexes that they have 1:2 M:L (metal:ligand) ratio. The Fe(III), Cu(II) and Zn(II) complexes, $[Fe(HL)(L)(H_2O)_2](ClO_4)_2$, $[Cu(HL)_2](ClO_4)_2{\cdot}3H_2O$, $[Zn(HL)_2](ClO_4)_2{\cdot}H_2O$ are 2:1 electrolytes whereas the Co(II) complex, $[Co(HL)(L)(H_2O)]ClO_4{\cdot}H_2O$, is 1:1 electrolyte according to the molar conductivity data.

KEY WORDS: Hydrazine, Hydroxybenzylidene, Benzamide, Metal Complexes, Crystal Structure

INTRODUCTION

Benzamide and its analogues have various application in synthesis of heterocyclic ring skeletons and are used as intermediate in the synthesis of 2,3-disubstituted quinazolin-4(3H)-one heterocycles [1]. In addition, benzamides are identified as important structural unit present in many compounds having potential biological activities, which are extracted from natural sources. For example, molecules, like proteins which play an essential role in almost all biological processes such as enzymatic catalysis (nearly all known enzymes are proteins), transport/storage (haemoglobin), immune protection (antibodies) and mechanical support (collagen). The benzamide derivatives are also useful for modulation of numerous metabolic functions including regulation of carbohydrate, protein and lipid metabolism, regulation of normal growth and/or development, influence on cognitive function, resistance to stress and mineralocorticoid activity [2, 3].

The hydrazones constitute an important class of biologically active molecules, which have attracted attention of medicinal chemists due to their wide ranging pharmacological properties and their potential application as antitumor, antiviral and antiinflammatory agents [4-9]. For example, several hydrazones and hydrazides of isoniazid had shown good activity against tubercular, fungal, bacterial and mycobacterial infections [10-15]. Some of hydrazones exhibited potential *in vitro* leishmanicidal activity [16]. It was reported that substituted N'-(2-oxoindolin-3-ylidene)-benzohydrazides, isatin derivatives, had apoptosis inducers as potential

*Corresponding author. E-mail: atavman@istanbul.edu.tr

anticancer agents. Apoptosis, or programmed cell death, plays a crucial role in normal cell development and tissue homeostasis [17].

Structural characterization of benzohydrazides is important to comprehend their effect mechanisms because of their considerable biological effects. Recently, the crystal structures of hydrazone compounds have been widely studied [18-21].

In our previous study, the crystal structure of 2-amino-*N*'-[(1*Z*)-1-(4-chlorophenyl)-ethylidene]benzohydrazide was reported [22]. The structure of the compound also was characterized by elemental analysis, MS, FT-IR and NMR spectroscopic techniques. In this study, we synthesized and characterized *N*-(2-{[(2*E*)-2-(2-hydroxybenzylidene)hydrazinyl]-carbonyl}phenyl)benzamide (**HL**, Figure 1), a new benzohydrazide derivative, and its Co(II), Fe(III), Cu(II) and Zn(II) complexes. The structure of the compounds is characterized by the analytical data and FT-IR, FT-Raman, NMR spectroscopy. TGA, magnetic moment and molar conductivity measurements were carried out for the complexes. In addition, the crystal structure of **HL** is determined by X-ray diffraction analysis.

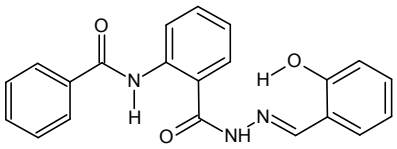

Figure 1. The chemical structure of the ligand (**HL**).

EXPERIMENTAL

Chemicals and apparatus

All chemicals and solvents were of reagent grade from Sigma-Aldrich, Merck, Alfa Easer, Carlo Erba and Acros Organics and they were used without further purification.

Elemental analysis data were obtained with a Thermo Finnigan Flash EA 1112 analyzer. Molar conductivity of the complexes was measured on a WTW Cond315i conductivity meter in DMF at 25 ºC. Magnetic moment measurements for the paramagnetic complexes were carried out on a Sherwood Scientific apparatus (MK1) at room temperature by Gouy's method. FT-IR spectra were recorded on a Bruker Optics Vertex 70 spectrometer using ATR (Attenuated Total Reflection) techniques. The FT-Raman spectra were also recorded in the same instrument with a R100/R RAMII Raman module equipped with Nd:YAG laser source operating at 1064 nm line with 200 mW power and a spectral resolution of ±2 cm^{-1}. Thermogravimetric (TG) study was made on a TG-60WS Shimadzu, with a heating rate of 10 ºC/min under flowing air at the rate of 50 mL/min. ^{1}H-NMR spectra were run on a Varian Unity Inova 500 NMR spectrometer in $CDCl_3$.

Synthesis of the compounds

*N-(2-{[(2E)-2-(2-Hydroxybenzylidene)hydrazinyl]carbonyl}phenyl)benzamide (**HL**)*. To the well stirred solution of salicylaldehyde (0.1 mL, 0.8196 mmol) in dry ethanol (10 mL) was added 2-3 drops of sulfuric acid (98%) and stirred with gentle heating for 30 min followed by addition of ethanolic solution of 2-phenyl-4*H*-3,1-benzoxazin-4-one (0.2 g, 7.84 mmol, Scheme 1). The mixture was further refluxed with continuous stirring for one hour; the progress of the reaction was monitored with TLC upon completion of the reaction. The mixture was allowed to cool to room temperature, and was then poured into ice cold water. The product precipitated was

filtered, washed with 5% cold $NaHCO_3$ solution, dried and recrystallized from ethanol (239 mg).

Yield: 81%, m.p.: 224-226 ^oC. Anal. calcd. for $C_{21}H_{17}N_3O_3$ (%): C, 70.18; H, 4.77; N, 11.69; found (%): C, 70.08; H, 5.07; N, 11.67. MW: 359.4 g/mol. MS (ESI), m/z (%): 358.2 ($[M-1]^+$, 100), 359.2 ($[M]^+$, 23.4), 393.7 (16.0), 420.7 (15.2), 340.1 (5.1), 240.2 (4.0). FT-IR (ATR, ν/cm^{-1}): 3284 br, 3198 m, 3054 m, 2849 w, 1667 m, 1650 m, 1605 m, 1519 m, 1450 m, 1282 m, 1254 m, 961 m, 875 m, 758 s, 699 m, 665 m, 617 m, 513 m, 445 w. FT-Raman (ν/cm^{-1}): 3068 w, 1659 m, 1609 s, 1574 m, 1554 m, 1487 m, 1452 m, 1295 m, 1242 m, 1173 m, 1032 m, 1004 m, 926 w, 897 w, 77 s. ^{1}H-NMR ($CDCl_3$) δ_H, ppm: 11.19 (s, 2H, –CO–NH–N=C, –CO–NH–Ph), 11.10 (s, 1H, OH), 9.17 (s, 1H, CH=N), 8.61 (d, 1H, *J*=8.4), 7.94 (d, 1H, *J*=7.3), 7.81 (dd, 2H, *J* = 8.5, 8.7), 7.68 (m, 3H), 7.49 (t, 1H, *J* = 8.0), 7.21 (d, 1H, *J* = 8.1), 7.12 (t, 2H, *J* = 7.6), 6.97 (d, 1H, *J* = 8.1), 6.93 (t, 1H, *J* = 8.4).

*[Fe(**HL**)(**L**)(H_2O)$_2$](ClO_4)$_2$.* 135 mg HL (0.375 mmol) and 173 mg $Fe(ClO_4)_3 \cdot 6H_2O$ (0.375 mmol) were dissolved in acetonitrile (20 mL) and the mixture was refluxed for 2 h. The mixture was filtered and kept at room temperature for slow evaporation. After 2 days, the black crystals were formed and filtered, dried at room temperature (150 mg).

Yield: 81%, m.p. 200-205 ^oC (explosion!). Anal. calcd. for $C_{42}H_{37}Cl_2CuN_6O_{16}$ (%): C, 50.02; H, 3.70; N, 8.33; Found (%): C, 50.44; H, 4.18; N, 9.26. MW: 1008.52 g/mol; μ_{eff} = 4.20 BM; Molar conductivity: 134 $\Omega^{-1}cm^2mol^{-1}$ (in DMF, 25±1 ºC). FT-IR (ATR, ν/cm^{-1}): 3322 m, br, 3223 m, br, 3065 m, br, 2997 w, 2859 w, 1736 m, 1641 m, 1604 m, 1587 m, 1515 m, 1448 m, 1384 m, 1300 m, 1258 m, 1105 s, 1052 s, 897 m, 755 m, 705 m, 621 s, 518 m, 432 m. Raman data could not be obtained. TGA (temperature, ^oC: weight loss, %): 100: 2.1; 150: 5.3; 200: 7.3; 219: explosion!

*[Co(**HL**)(**L**)(H_2O)]$ClO_4 \cdot H_2O$.* 135 mg HL (0.375 mmol) and 137 mg $Co(ClO_4)_2 \cdot 6H_2O$ (0.375 mmol) were dissolved in acetonitrile (20 mL) and the mixture was refluxed for 2 h. The mixture was filtered and kept at room temperature for slow evaporation. After 2 days, a brown precipitate was formed. This precipitate was filtered and dried at room temperature (147 mg).

Yield: 78%, m.p. 215 ^oC. Anal. calcd. for $C_{42}H_{37}ClCoN_6O_{12}$ (%): C, 55.30; H, 4.09; N, 9.21; Found (%): C, 56.25; H, 4.62; N, 9.68. MW: 912.10 g/mol. μ_{eff} = 3.31 BM. Molar conductivity: 87 $\Omega^{-1}cm^2mol^{-1}$ (in DMF, 25±1 ºC). FT-IR (ATR, ν/cm^{-1}): 3325 w, 3235 m, br, 3062 m, br, 3003 w, br, 2850 w, br, 1736 m, 1682 m, 1604 m, 1590 m, 1522 m, 1448 m, 1389 m, 1325 w, 1275 m, 1118 m, 1054 s, 895 m, 761 s, 688 s, 621 s, 515 m, 423 m. Raman data could not be obtained. TGA (temperature, ^oC: weight loss, %): 100: 2.1; 150: 3.05; 200: 3.7; 250: 13.05; 300: 23.2; 350: 42.4; 400: 51.1; 450: 54.3; 500: 57.1; 550: 69.5; 600: 92.2; 650: 92.7 (CoO%: 8.38).

*[Cu(**HL**)$_2$](ClO_4)$_2 \cdot 3H_2O$.* 135 mg HL (0.375 mmol) and 140 mg $Cu(ClO_4)_2 \cdot 6H_2O$ (0.375 mmol) were dissolved in acetonitrile (20 mL). A green turbidity was formed instantly. This mixture was refluxed for 2 h, then cooled to room temperature and filtered. The green precipitate was dried at room temperature (155 mg).

Yield: 80%, m.p. 273 ^oC (explosion!). Anal. calcd. for $C_{42}H_{40}Cl_2CuN_6O_{17}$ (%): C, 48.73; H, 3.89; N, 8.12; Found (%): C, 48.13; H, 3.49; N, 8.11. MW: 1035.25 g/mol. μ_{eff} = 1.56 BM. Molar conductivity: 142 $\Omega^{-1}cm^2mol^{-1}$ (in DMF, 25±1 ºC). FT-IR (ATR, ν/cm^{-1}): 3361 m, 3187 w,br, 3062 m,br, 2888 w,br, 1679 m, 1627 m, 1604 m, 1582 m, 1554 m, 1509 s, 1445 m, 1393 m, 1336 m, 1275 m, 1216 m, 1152 m, 1074 m, 1040 s, 904 m, 744 m, 694 m, 621 m, 535 m, 443 m. Raman data could not be obtained. TGA (temperature, ^oC: weight loss, %): 100: 4.2; 150: 4.4; 200: 4.4; 270: explosion!

*[Zn(**HL**)$_2$](ClO_4)$_2 \cdot H_2O$.* 135 mg HL (0.375 mmol) and 140 mg $Zn(ClO_4)_2 \cdot 6H_2O$ (0.375 mmol) were dissolved in acetonitrile (20 mL). A slightly yellow turbidity was formed at one minute.

This mixture was refluxed for 2 h, then cooled to room temperature and filtered. The dirty white precipitate was dried at room temperature (140 mg).

Yield: 74%, m.p. 180-194 ^{o}C. Anal. calcd. for $C_{42}H_{36}Cl_2N_6O_{15}Zn$ (%): C, 50.39; H, 3.62; N, 8.39; Found (%): C, 50.33; H, 4.25; N, 8.39. MW: 1001.08 g/mol; Molar conductivity: 110 $\Omega^{-1}cm^2mol^{-1}$ (in DMF, 25±1 ºC). MS (ESI): 781.2 ([(Zn+2HL)-3]$^+$, 100%), 783.2 ([(Zn+2HL)-1]$^+$, 70.6%), 785.2 ([(Zn+2HL)+1]$^+$, 56.0%), 786.2 ([(Zn+2HL+2)]$^+$, 28.8%), 719.3 ([(2HL)+1]$^+$, 17.6%), 360.2 ([HL+1]$^+$, 58.8%), 422.0 ([(HL+Zn)-3]$^+$, 44.1%), 424.0 ([(HL+Zn)-1]$^+$, 32.1%). FT-IR (ATR, ν/cm^{-1}): 3342 m, br, 3266 m, 3095 w, br, 2883 w, br, 1686 m, 1666 m, 1616 m, 1590 m, 1560 m, 1518 m, 1448 m, 1398 m, 1280 m, 1110 m, 1074 m, 1038 s, 976 m, 756 s, 705 m, 619 m, 591 m, 515 m. FT-Raman (ν/cm^{-1}): 3076 w, 1667 w, 1611 s, 1589 m, 1561 m, 1455 m, 1326 m, 1281 m, 1168 m, 1138 m, 1052 w, 1003 w, 936 m, 89 m. ^{1}H-NMR ($CDCl_3$) δ_C, ppm: 11.94 s, br (1H, OH), 11.69 s, br (1H, –CO–NH–N=C), 11.10 (s, br, 1H, 1H, –CO–NH–Ph), 9.64 s, br (1H, CH=N), 8.71 d (1H, J=7.8), 8.47 s, br (1H), 8.06 d (2H, J = 6.8), 7.58 m (5H), 7.07 d, br (1H, J = 9.7), 6.97 t (3H, J = 6.83, 7.32). TGA (temperature, ^{o}C: weight loss, %): 100: 1.6; 150: 2.1; 200: 2.9; 250: 7.8; 300: 20.0; 350: 35.5; 400: 46.1; 450: 49.0; 500: 52.4; 550: 55.3; 600: 79.3; 650: 89.8; 700: 91.3 (ZnO%: 8.0).

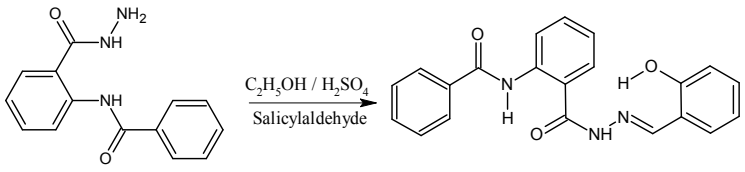

Scheme 1. Synthesis of *N*-(2-{[(2E)-2-(2-hydroxybenzylidene)hydrazino]carbonyl}phenyl) benzamide (**HL**).

Crystallography

Suitable crystal was selected for data collection which was performed on a Bruker SMART APEX CCD area-detector diffractometer with graphite monochromated Mo-*Kα* radiation (λ = 0.71073 Å) at 25±1 ^{o}C (298 K). The structures were solved by direct methods using SHELXS-97 and refined by full-matrix least-squares methods on F using SHELXL-97 [23]. All non-hydrogen atoms were refined with anisotropic parameters. The H atoms of C atoms were located from different maps and then treated as riding atoms with C–H distances of 0.96 – 0.97 Å. H atoms treated by a mixture of independent and constrained refinement. For the structure solution, 9402 reflections were collected, 3530 were unique (R_{int} = 0.066); equivalent reflections were merged. Lorentz-polarization and absorption corrections were applied using Bruker SAINT [24] and SADABS [25] software. The crystal structure was deposited at the Cambridge Crystallographic Data Centre under the following deposition number: CCDC 1538433.

RESULTS AND DISCUSSIONS

Discussion of the ligand structure

Synthesis of the ligand (**HL**) was given in Scheme 1. The structure of **HL** was confirmed by the characteristic absorption peaks of amide in IR region, D_2O exchangeable amide proton peak in the ^{1}H-NMR region and further confirmation was done on the basis of molecular ion peak in EI-MS, FAB-MS and Mass fragmentation pattern. It is important to note that **HL** did not cyclize further under the selected reaction conditions.

In addition to spectroscopic proof of the structure, crystals of **HL** were obtained and the absolute structure was determined with the help of X-ray crystallography, which confirmed the formation and reactivity of the open chain products.

The crystal data and details of data processing are given in Table 1. Table 2 contains the hydrogen bond geometry parameters. Selected bond lengths and angles are given in Table 3; some torsion angles are given in Table 4. The ORTEP III drawing of **HL** is given in Figure 2 and the unitcell packing diagram with the intermoleculer H-bonding is given in Figure 3.

Table 1. Crystal and experimental data and refinement of the crystal structure of **HL**.

Empirical formula	$C_{21}H_{17}N_3O_3$
Formula weight (g/mol)	359.38
Crystal system, Space group	Monoclinic, *C*2/*c*
Color, habit	Colorless, block
Unit cell dimensions (Å, °)	a = 21.191(17), b = 8.308 (7) c = 22.333 (18), β = 113.093 (16)
Cell volume (Å^3)	3617 (5)
Z, $d_{calc.}$ (g/cm^3)	8, 1.320
F(000)	1504
Crystal size (mm)	0.43 × 0.42 × 0.12
Linear abs. coefficient (μ, mm^{-1})	0.09
No. of observations (I>2.00 σ (I))	1574
Refinement method	Full-matrix least-squares on F
Goodness of fit indicator	0.98
Index ranges	$-26 \le h \le 25$, $-7 \le k \le 10$, $-27 \le l \le 27$
θ range for data collection (°)	1.9 – 26.0
Data collection	SMART
R [$F^2 > 2\sigma(F^2)$]	0.058
$wR(F^2)$	0.144
Largest diff. peak and hole (e$^-$/Å^3)	0.15 and -0.14

Table 2. Hydrogen-bond geometry (Å, °)

D–H···*A*	*D*–H	H···*A*	*D*···*A*	*D*–H···*A*
N1–H1A···O2	0.85(3)	1.97(2)	2.707(4)	144(2)
O3–H3A···N3	0.83(3)	1.85(3)	2.597(4)	149(3)
N2–H2A···O1^{i}	0.87(3)	1.99(3)	2.837(4)	164(3)
C4–H4···O3^{ii}	0.93	2.60	3.399(5)	145
C17–H17···O2^{iii}	0.93	2.46	3.291(5)	149

Symmetry codes: (i) x+3/2, y+1/2, z; (ii) −x+1/2, −y+1/2, −z; (iii) x, y−1, z.

There are two intra- and three inter-molecular hydrogen bonds in the **HL** molecule (Table 2). The intermolecular hydrogen bonding distances are 1.99, 2.60 and 2.46 Å, for N2–H2A···O1, C4–H4···O3 and C17–H17···O2, respectively. The intermolecular H-bonding values for C4–H4···O3 and C17–H17···O2 (2.60 and 2.46 Å, respectively) are higher than the ordinary intermolecular H-bonding lengths as expected due to very weak electron-withdrawing characteristic of the aromatic CH hydrogen atoms. The crystal structure is stabilized by the intermolecular hydrogen bondings. The intramolecular hydrogen bonding distances, (N1–H1A···O2: 1.97(2) Å; O3–H3A···N3: 1.85(3) Å), are in agreement with the literature data [21, 26-30]. The intramolecular hydrogen bonds cause forming almost two more rings in the molecule. It is expected that the intramolecular hydrogen bonds affect the physical properties of HL, significantly. It is not a very common feature that there are hydrogen bonds in a molecule more than one.

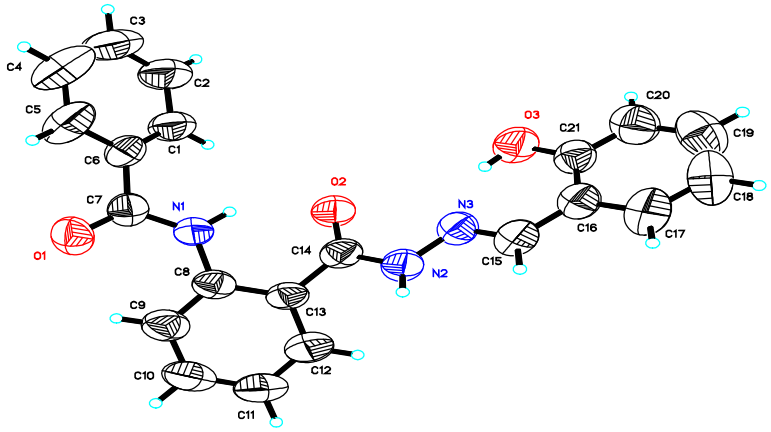

Figure 2. The ORTEP III drawing of **HL**.

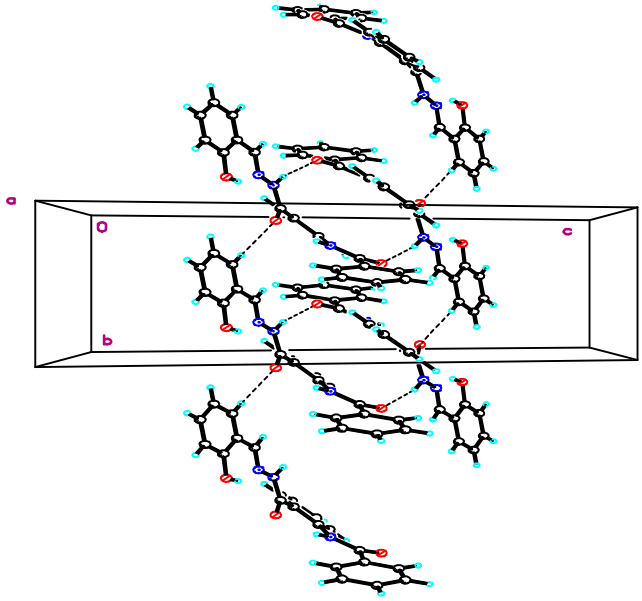

Figure 3. The ORTEP III drawing of **HL** showing the stability *via* hydrogen bonding between the molecules.

The major torsion angles: C1-C6-C7-N1: 25.0(4); C7-N1-C8-C9: 20.4(4); C12-C13-C14-N2: -36.1(3); N3-C15-C16-C17: -178.8(2)º (Table 4). According to the torsion angles, the benzamide ring is twisted by 25º according to the phenyl ring at the middle of **HL** whereas the phenyl ring is twisted by the angle of 36.1º compared to the benzamide ring. Some of the considerable bond lengths are: C6-C7-N1: 115.2(2); C7-N1-C8: 129.3(2); C13-C14-N2: 115.0(2); C14-N2-N3: 118.5(2); N2-N3-C15: 118.0(2); N3-C15-C16: 120.5(3)º. The bond angles at the bridging parts between three rings are varying at the 115.0 – 129.3º range (Figure 3).

Table 3. Selected bond lengths (Å) and angles (º)

Bond lengths, Å			
O1–C7	1.231(3)	O3–H3A	0.828(10)
O2–C14	1.229(3)	N1–C7	1.346(3)
O3–C21	1.350(3)	N1–C8	1.403(3)
N1–H1A	0.855(10)	N2–C14	1.349(3)
N3–C15	1.274(3)	N2–N3	1.370(3)
C1–C6	1.350(3)	C5–C6	1.363(4)
C6–C7	1.489(4)	C10–C11	1.370(4)
C11–C12	1.377(4)	C13–C14	1.476(4)
C15–C16	1.442(4)	C9–H9	0.9300
Bond angles, º			
C21–O3–H3A	106(2)	C15–N3–N2	118.0(2)
C7–N1–C8	129.3(2)	O2–C14–N2	121.5(3)
C14–N2–N3	118.5(2)	N2–C14–C13	115.0(2)
O2–C14–C13	123.5(3)	N3–C15–C16	120.5(3)
O1–C7–N1	123.1(3)	O1–C7–C6	121.7(3)
N1–C7–C6	115.2(2)	C1–C6–C7	123.1(3)
C9–C8–N1	123.1(3)	C13–C8–N1	117.9(2)
O3–C21–C16	123.3(3)	O3–C21–C20	116.5(3)

The C=O bond lengths are very close to each other: 1.231(3) and 1.229(3) Å for C7–O1 and C14–O2, respectively. The C–OH (C21–O3) bond length (1.350(3)) is higher than the average length of C=O bond as expected. The C7–N1 bond length (1.346(3) Å) is shorter than that of the C8–N1 (1.403(3) Å) due to the C7 carbon atom bonded to the carbonyl oxygen atom (O=C7–N1). Oxygen atom makes the C7–N1 bond shorter than C8–N1 because of its electron-withdrawing characteristic. The C14–N2 and C15–N3 bond lengths are 1.349(3) Å and 1.274(3) Å, respectively. It is obvious that the second one is a double bond. The bond length of N2–N3 is 1.370(3) Å and it is a single bond as expected.

Table 4. Selected torsion angles (º)

C14-N2-N3-C15	174.5(2)	C12-C13-C14-O2	143.3(3)
N1-C8-C13-C14	1.4(3)	N3-N2-C14-O2	-3.7(4)
N3-N2-C14-C13	175.8(2)	C12-C13-C14-N2	-36.1(3)
C8-C13-C14-N2	145.7(2)	C1-C6-C7-N1	25.0(4)
C7-N1-C8-C13	-161.0(2)	N3-C15-C16-C17	-178.8(2)
N2-N3-C15-C16	177.0(2)	C5-C6-C7-N1	-156.9(2)
C7-N1-C8-C9	20.4(4)		

Properties of the complexes

Molar conductivity data of the complexes give useful information about the structure of the complexes. According to the molar conductivity data, the Fe(III), Cu(II) and Zn(II) complexes (110 – 142 $\Omega^{-1}cm^2mol^{-1}$) are considered as 1:2 and the Co(II) complex is acceptable as 1:1 (87 $\Omega^{-1}cm^2mol^{-1}$). According to Geary, molar conductivity values for 1:1 and 1:2 electrolyte in DMF generally fall between 65 – 90 and 130 – 170 $\Omega^{-1}cm^2mol^{-1}$, respectively [31]. Elemental analysis and molar conductivity data shows that one of the ligands releases a phenolic hydrogen in the Co(II) complex and $[Co(HL)(L)(H_2O)]ClO_4 \cdot H_2O$ is suggested for the empirical formula of the Co(II) complex.

Room temperature magnetic moment values (μ_{eff}) of the paramagnetic complexes are 1.65, 4.20 and 3.31 BM for the Cu(II), Fe(III) and Co(II) complexes, respectively. Magnetic moment value of Cu(II) complex (1.65 BM) is in the expected range for a typical mononuclear d^9 Cu(II)

complex. The room temperature effective magnetic moment value of the Fe(III) complex indicates stabilization of the species having intermediate ferric spin (S = 3/2) state. The occurrence of such an intermediate spin state is typical for the six and five coordinate ferric complexes [32-34]. The room temperature magnetic moment value of Co(II) complex, 3.31 BM, lower than the spin-only value for high spin and higher than the spin-only value for low spin configurations. This may be considered as a spin equilibrium between two spin states [35] and it can be attributed a square pyramidal geometry for this complex nearly [36, 37].

The experimental data of the Co(II) and Fe(III) complexes suggest us monodeprotonated structure in contradistinction to the Cu(II) and Zn(II) complexes. The dark color of the complexes, especially the Fe(III) and Co(II) complexes, shows that there are charge transfer transitions ligand to metal ions through phenolic oxygen atom, O→M [38, 39].

Thermogravimetric analysis

The major features of the thermal analysis of the complexes are given in Experimental section. TGA curves of the Co(II) and Zn(II) complexes are given in Figure 4. The decomposition points of the complexes are in the 180 – 273 ^{o}C range. In this range, explosions were occurred in the Fe(III) and Cu(II) complexes due to presence of the perchlorate anion. Because of the explosion, TGA analysis could not be performed for these complexes fully. However, we could detect the coordinated and uncoordinated water molecules in the complexes by means of TGA. The uncoordinated lattice water molecules were lost through evaporation from 50 to 100 ºC (dehydration) in the Cu(II) and Zn(II) complexes whereas the coordinated water molecules (aqua) were removed at temperatures near 150 ºC in the Fe(III) and Co(II) complexes. The full TGA data of the Co(II) and Zn(II) complexes could be obtained without explosion (Figure 4) between 40 and 800 ^{o}C.

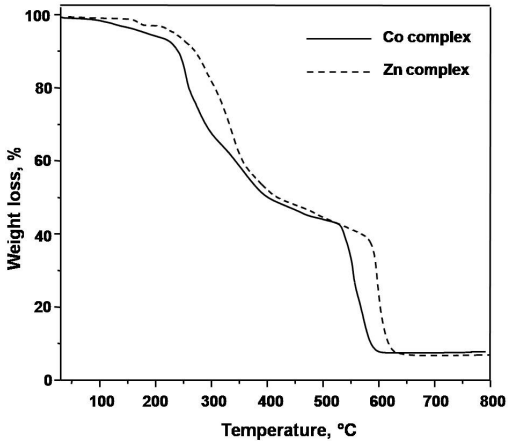

Figure 4. TGA curves of the Co(II) and Zn(II) complexes.

Thermal degradation of the complexes occurred at three stages. Firstly, uncoordinated lattice water left at the 50 – 100 ºC range as mentioned above. At the second stage, a considerable weight losses observed between 200 and 400 ºC can be explained in terms of cleavage of hydroxyl, NHs and carbonyl groups. Above 500 ºC, all other organic parts of complexes are oxidized to carbon dioxide and water. Complete decomposition of the complexes continues up to 600 ºC probably to the forming of MO. Molecular weight ratio of the amount of metal oxide shows very good agreement for the proposed structures according to the TGA data in the Co(II) and Zn(II) complexes.

^{1}H-NMR Spectra

^{1}H-NMR spectral data of the ligand and the Zn(II) complexes are given in Experimental Section. The phenolic OH and CH=N protons give singlet at 11.10 and 9.17 ppm, respectively, in the ligand. In the Zn(II) complex, the OH signal shifted to 11.94 ppm from 11.10 ppm; the CH=N proton shifted to 9.64 ppm from 9.17 ppm with respect to the ligand. These data showed that the phenolic OH oxygen and the CH=N nitrogen atoms coordinated to the Zn(II) ion, and the OH proton did not remove on complexation (The other data such as elemental analysis, molar conductivity, also confirm that the OH proton does not remove on complexation). The hydrazine (–CO–NH–N=C) and benzamide (–CO–NH–Ph) NH protons of the ligand appear at 11.19 ppm as a singlet, respectively. These NH protons exhibit different behavior in the Zn(II) complex: The NH proton of hydrazine that neighbor to the coordinated imine nitrogen (–N<u>H</u>–CH=N) gives a singlet at 11.69 (from 11.19), whereas the benzamide NH proton (far from the coordinated imine nitrogen) is slightly affected from coordination (it gives a singlet at 11.10 ppm). This observation is considered as an additional evidence for CH=N nitrogen atom coordination.

Vibrational Spectroscopy

FT-IR and FT-Raman spectral data of the compounds are given in Experimental section. The FT-IR spectra of the ligand and the complexes are given in Figure 5. FT-Raman spectra of HL and the Zn(II) complex were shown in Figure 6. We could not get the FT-Raman spectra of the Cu(II), Co(II) and Fe(III) complexes (Raman inactive).

In the IR spectra of the ligand, the medium bands at 1650 and 1667 cm^{-1} must belong to the C=O groups. The corresponding wavenumbers in the complexes are detected at the 1617 – 1736 cm^{-1} range. In the Raman spectra, the 1653 cm^{-1} and 1667 cm^{-1} bands can be assigned for the ν(C=O) group of the ligand and the Zn(II) complex, respectively. The medium (IR) and strong (Raman) bands between 1604 – 1616 cm^{-1} are attributed to the aromatic ring ν(C=C) frequencies. There are no considerable changes in these frequencies on complexation as expected. Similarly the (C=N) asymmetric stretching frequency of the ligand is appeared at 1519 cm^{-1}, and it was detected at the 1582 – 1590 cm^{-1} range in the complexes. This considerable shifting shows that the coordination occurs through the C=N nitrogen atom.

The strong bands between 761 and 744 cm^{-1} (in the ligand: 758 cm^{-1}), and the strong or medium bands at the 830 – 730 cm^{-1} range are due to the out-of-plane deformation bands for the aromatic C–Hs. The bands at 3284 cm^{-1} (w, br) and 3198 cm^{-1} (m, br) can be attributed to ν(OH) and ν(NH) in the ligand, respectively. These bands shifted to the 3322 – 3361 cm^{-1} and 3187 – 3266 cm^{-1} ranges in the complexes, respectively.

In the FT-IR spectra of all the complexes, the new strong band between 1105 and 1152 cm^{-1} can be assigned to the stretching vibrations of the uncoordinated perchlorate anion, ν(Cl=O). In addition, the medium bands in the complexes near 620 cm^{-1} are due to ν_4 mode of perchlorate anion [40-42].

The broad band between 3000-2500 cm^{-1} in the complexes should be belonged to the hydrogen bonding because of the coordinated and uncoordinated (lattice) water molecules. The characteristic ν(C–H) modes of ring residues are observed in the range of 3054 – 3095 cm^{-1}, in the FT-IR and FT-Raman spectra of the compounds (Figures 5 and 6).

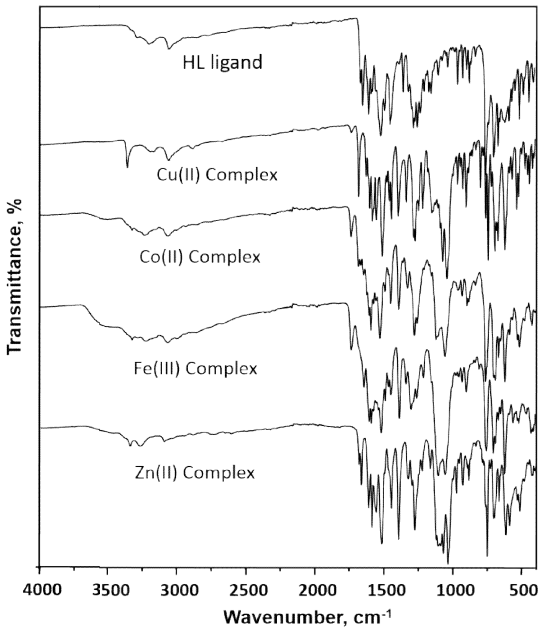

Figure 5. FT-IR spectra of **HL** and its complexes.

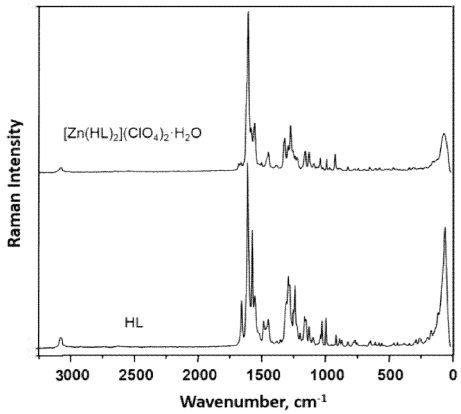

Figure 6. FT-Raman spectra of **HL** and its Zn(II) complex.

CONCLUSION

Benzamide and its analogues have various applications in synthesis of heterocyclic ring skeletons and are used as intermediate in the synthesis of some heterocycles. In addition, some benzamide derivatives can be extracted from plants having potential biological activities.

In this study, a new benzamide derivative, *N*-(2-{[(2*E*)-2-(2-hydroxybenzylidene)-hydrazinyl]carbonyl}phenyl)-benzamide (**HL**) and its complexes with $Co(ClO_4)_2$, $Fe(ClO_4)_3$, $Cu(ClO_4)_2$ and $Zn(ClO_4)_2$ were synthesized and characterized. In addition, the crystal structure of **HL** is determined by X-ray diffraction at room temperature. According to the analytical and spectral data, **HL** behaves as a bidentate in the chelate complexes; and the complexes have 1:2 M:L ratio. According to the molar conductivity measurements in DMF, the Fe(III), Cu(II) and Zn(II) complexes are 2:1 electrolytes whereas the Co(II) complex can be considered as 1:1 electrolyte.

As a conclusion, the structures in Figure 7 can be proposed for the complexes. It can be proposed a tetrahedral geometry for the Cu(II) and Zn(II) complexes; distorted octahedral and square pyramidal geometries for the Fe(III) and Co(II) complexes, respectively [43-47]. In addition, the ball-stick structure for the Cu(II) and Zn(II) complexes is shown in Figure 8.

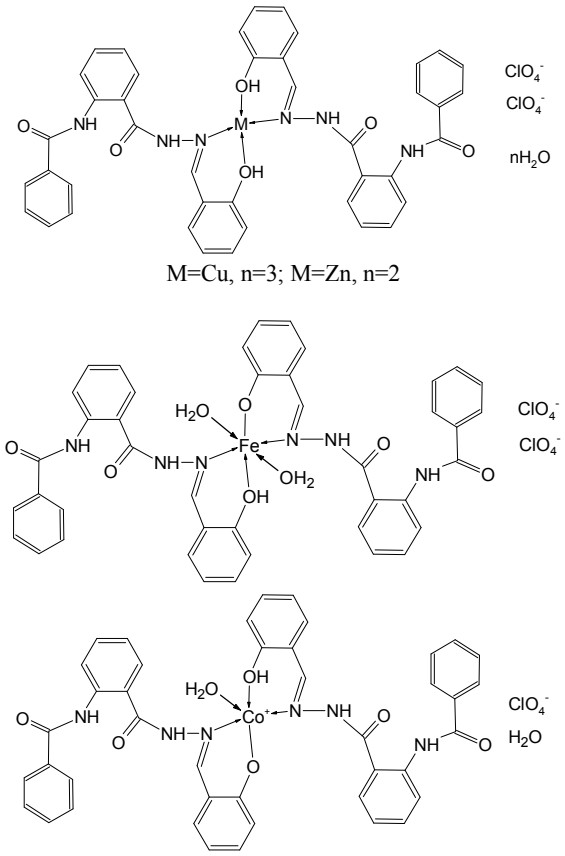

Figure 7. The proposed structures for the complexes.

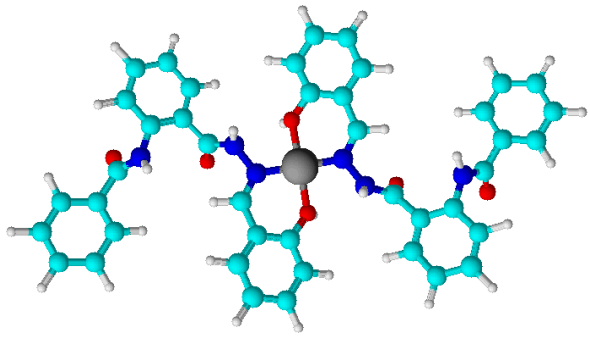

Figure 8. The ball-stick structure for the Cu(II) and Zn(II) complexes (the structures were obtained by ACD/ChemSketch software program (the H_2O molecules and the perchlorate anions are omitted).

ACKNOWLEDGEMENT

This work was supported by the Scientific Research Projects Unit of Istanbul University and TUBITAK-BIDEB.

REFERENCES

1. Acton, Q.A. *Benzoic Acids – Advances in Research and Application*, 2013 Edition, Scholarly Editions: Atlanta, USA; **2013**.
2. Powers, J.; Rew, P.Y.; Yan, X. Benzamide derivatives and uses related thereto. *US* 7659287 B2; **2010**.
3. Mao, W.; Ning, M.; Liu, Z.; Zhu, Q.; Leng, Y.; Zhang, A. Design, synthesis, and pharmacological evaluation of benzamide derivatives as glucokinase activators. *Bioorg. Med. Chem.* **2012**, 20, 2982-2991.
4. Jimenez-Pulido, S.B.; Linares-Ordonez, F.M.; Martinez-Martos, J.M.; Moreno-Carretero, M.N.; Quiros-Olozabal, M.; Ramirez-Exposito, M.J. Metal complexes with the ligand derived from 6-acetyl-1,3,7-trimethyllumazine and benzohydrazide. Molecular structures of two new Co(II) and Rh(III) complexes and analysis of in vitro antitumor activity. *J. Inorg. Biochem.* **2008**, 102, 1677-1683.
5. Rollas, S.; Küçükgüzel, Ş.G. Biological activities of hydrazone derivatives. *Molecules* **2007**, 12, 1910-1939.
6. Abadi, A.H.; Eissa, A.A.H.; Hassan, G.S. Synthesis of novel 1,3,4-trisubstituted pyrazole derivatives and their evaluation as antitumor and antiangiogenic agents. *Chem. Pharm. Bull.* **2003**, 51, 838-844.
7. Terzioğlu, N.; Gürsoy, A. Synthesis and anticancer evaluation of some new hydrazone derivatives of 2,6-dimethylimidazo[2,1-b][1,3,4]thiadiazole-5-carbohydrazide. *Eur. J. Med. Chem.* **2003**, 38, 781-786.
8. Todeschini, A.R.; Miranda, A.L.; Silva, C.M.; Parrini, S.C.; Barreiro, E.J. Synthesis and evaluation of analgesic, antiinflammatory and antiplatelet properties of new 2-pyridylarylhydrazone derivatives. *Eur. J. Med. Chem.* **1998**, 33, 189-199.
9. Abdel-Aal, M.T.; El-Sayed, W.A.; El-Ashry, E.H. Synthesis and antiviral evaluation of some sugar arylglycinoylhydrazones and their oxadiazoline derivatives. *Arch. Pharm. Chem. Life Sci.* **2006**, 339, 656-663.
10. Joshi, S.D.; Vagdevi, H.M.; Vaidya, V.P.; Gadaginamath, G.S. Synthesis of new 4-pyrrol-1-yl benzoic acid hydrazide analogs and some derived oxadiazole, triazole and pyrrole ring

systems: a novel class of potential antibacterial and antitubercular agents. *Eur. J. Med. Chem.* **2008**, 43, 1989-1996.
11. Shah, R.R.; Mehta, R.D.; Parikh, A.R. Studies on isoniazide derivatives: preparation and antimicrobial activity of 2-aryl-3-(pyridylcarbomyl)-5-carboxymethyl-4-thiazolidinones. *J. Indian Chem. Soc.* **1985**, 62, 255-257.
12. Vigorita, M.G.; Maccari, R.; Ottana, R.; Monforte, F. Synthesis and antiinflammatory, analgesic activity of 3,3′-(1,2-ethanediyl)-bis[2-aryl-4-thiazolidinone] chiral compounds. Part 10. *Bioorg. Med. Chem. Lett.* **2001**, 11, 2791-2794.
13. Küçükgüzel, Ş.G.; Rollas, S.; Küçükgüzel, I.; Kiraz, M. Synthesis and antimycobacterial activity of some coupling products from 4-aminobenzoic acid hydrazones. *Eur. J. Med. Chem.* **1999**, 34, 1093-1100.
14. Cocco, M.T.; Congiu, C.; Onnis, V.; Pusceddo, M.C.; Schivo, M.L.; De Logu, A. Synthesis and antimycobacterial activity of some isonicotinoylhydrazones. *Eur. J. Med. Chem.* **1999**, 34, 1071-1076.
15. Sriram, D.; Yogeeswari, P.; Madhu, K.; Synthesis and in vitro and in vivo antimycobacterial activity of isonicotinoyl hydrazones. *Bioorg. Med. Chem. Lett.* **2005**, 15, 4502-4505.
16. Khan, K.M.; Zia-Ullah, M.R.; Hayat, S.; Kaukab, F.; Atta-ur-Rahman, M.I.C.; Perveen, S. Synthesis and *in vitro* leishmanicidal activity of some hydrazides and their analogues. *Bioorg. Med. Chem*. **2003**, 11, 1381-1387.
17. Sirisoma, N.; Pervin, A.; Drewe, J.; Tseng, B.; Cai, S.X. Discovery of substituted *N'*-(2-oxoindolin-3-ylidene)benzohydrazides as new apoptosis inducers using a cell- and caspase-based HTS assay. *Bioorg. Med. Chem. Lett.* **2009**, 19, 2710-2713.
18. Weng, Q.; Zhao, L. 2-Chloro-*N'*-(2-hydroxy-4-methoxybenzylidene) benzohydrazide. *Acta Cryst.* **2009**, E65, o808.
19. Fun, H.K.; Jebas, S.R.; Sujith, K.V.; Patil, P.S.; Kalluraya, B.; *N'*-[(*Z*)-4-(Dimethylamino)benzylidene]-4-nitrobenzohydrazide monohydrate. *Acta Cryst.* **2008**, E64, o1907-o1908.
20. Ali, H.M.; Zuraini. K.; Jefrey, B.W.; Ng, S.W. 1-(2,4-Dihydroxyphenyl)ethanone [(1*H*-indol-3-yl)acetyl]hydrazone-2-(1*H*-indol-3-yl)acetohydrazide (1/1). *Acta Cryst.* **2007**, E63, o1729-o1730.
21. Zhi, F.; Yang, Y.L. 6-Chloro-*N'*-(2,4-dichlorobenzylidene)nicotinohydrazide. *Acta Cryst.* **2007**, E63, o4471.
22. Arfan, M.; Khan, R.; Tavman, A.; Saba, S. Spectral characterization and crystal structure of 2-amino-*N'*-[(1*Z*)-1-(4-chlorophenyl)ethylidene]-benzohydrazide. *J. Saud. Chem. Soc.* **2012**, 20, 40-44.
23. Sheldrick, G.M. A short history of *SHELX. Acta Crystallogr. Sect. A* **2008**, 64, 112–122.
24. Sheldrick, G.M. *SADABS Program for Empirical Absorption Correction*, University of Gottingen: Germany; **1996**.
25. Bruker. *SAINT-V6.28A Data Reduction Software*, Bruker AXS Inc.: Madison, WI, USA; **2001**.
26. Ban, H.-Y.; Li, C.-M. (*E*)-*N'*-(2-Chloro-5-nitrobenzylidene)-4-methoxybenzohydrazide. *Acta Cryst.* **2008**, E64, o2177.
27. He, Y.-Z.; Liu, D.-Z. (*E*)-*N'*-(4-Benzyloxy-3-methoxybenzylidene)benzohydrazide. *Acta Cryst.* **2005**, E61, o3855-o3856.
28. Jing, Z.-L.; Wang, X.-Y.; Chen, X.; Deng, Q.-L. *N'*-(2,4-Dichlorobenzylidene)-benzohydrazide. *Acta Cryst.* **2005**, E61, o4316-o4317.
29. Shan, S.; Tian, Y.-L.; Wang, S.-H.; Wang, W.-L.; Xu, Y.-L. (*E*)-*N'*-[1-(4-Aminophenyl)ethylidene]benzohydrazide. *Acta Cryst.* **2008**, E64, o1363.
30. Zhen, X.-L., Han, J.-R. (*E*)-*N'*-(4-Butoxy-3-methoxybenzylidene)benzohydrazide. *Acta Cryst.* **2005**, E61, o4282-o4284.

31. Geary, W. The use of conductivity measurements in organic solvents for the characterisation of coordination compounds. *J. Coord. Chem. Rev.* **1971**, 7, 81-122.
32. Tavman, A.; Agh-Atabay, N.M.; Güner, S.; Gücin, F.; Dülger, B. Investigation of Raman, FT-IR, EPR spectra and antimicrobial activity of 2-(5-H/Me/Cl-1*H*-benzimidazol-2-yl)-phenol ligands and their $Fe(NO_3)_3$ complexes. *Transit. Met. Chem.* **2007**, 32, 172-179.
33. El-Sawaf, A.K.; West, D.X.; El-Bahnasawy, R.M.; El-Saied, F.A. Synthesis, magnetic and spectral studies of iron(III) and cobalt(II,III) complexes of 4-formylantipyrine N(4)-substituted thiosemicarbazones. *Transit. Met. Chem.* **1998**, 23, 227-232.
34. Padhye, S.; Kauffman, G.B. Transition metal complexes of semicarbazones and thiosemicarbazones. *Coord. Chem. Rev.* **1985**, 63, 127-160.
35. Barefield, E.K.; Busch, D.H.; Nelson, S.M. Iron, cobalt, and nickel complexes having anomalous magnetic moments. *Quart. Rev. Chem. Soc.* **1968**, 22, 457-498.
36. Sacconi, L. Five coordination in 3d metal complexes. *Pure Appl. Chem.* **1968**, 17, 95-128.
37. Lippard, S.J. *Progress in Inorganic Chemistry*, Vol. 35, John Wiley and Sons, Inc.: Canada; **1987**; pp 599-600.
38. Tavman, A.; Agh-Atabay, M.N., Neshat, A.; Gucin, F.; Dulger, B.; Haciu, D. Structural characterization and antimicrobial activity of 2-(5-H/methyl/chloro-1*H*-benzimidazol-2-yl)-4-bromo/nitro-phenol ligands and their $Fe(NO_3)_3$ complexes. *Transit. Met. Chem.* **2006**, 31, 194-200.
39. Sun, Y.; Yi, L.; Yang, X.; Liu, Y.; Cheng, P.; Liao, D.; Yan, S.; Jiang, Z. Synthesis, crystal structures and properties of iron(III) complexes exhibited both high-spin and low-spin states within the crystal lattice. *Inorg. Chim. Acta* **2005**, 358, 396-402.
40. Gu, B.; Coates, J. D. *Perchlorate: Environmental Occurrence, Interactions and Treatment*, Springer Science + Business Media, Inc.: New York, USA; **2006**.
41. Nakamoto, K. *Infrared and Raman Spectra of Inorganic and Coordination Compounds*, Part B, 5th ed., John Wiley and Sons, Inc.: New York, USA; **1997**.
42. Tavman, A.; Ikiz, S.; Bagcigil, A. F.; Özgür, Y.; Ak, S. Spectral characterizations and antibacterial effect of 2-(5-R-1*H*-benzimidazol-2-yl)-4-methyl/bromo-phenols and some metal complexes. *Bull. Chem. Soc. Ethiop.* **2010**, 24, 391-400.
43. Taghizadeh, L.; Montazerozohori, M.; Masoudiasl, A.; Joohari, S.; White, J.M. New tetrahedral zinc halide Schiff base complexes: Synthesis, crystal structure, theoretical, 3D Hirshfeld surface analyses, antimicrobial and thermal studies. *Mater. Sci. Eng. C* **2017**, 77, 229-244.
44. Montazerozohori, M.; Masoudiasl, A.; Farokhiyani, S.; Joohari, S.; McArdle, P. Sonochemical synthesis of a new cobalt(II) complex: Crystal structure, thermal behavior, Hirshfeld surface analysis and its usage as precursor for preparation of CoO/Co_3O_4 nanoparticles. *Ultrason. Sonochem.* **2017**, 38, 134-144.
45. Masoudiasl, A.; Montazerozohori, M.; Naghiha, R.; Assoud, A.; McArdle, P.; Safi Shalamzari, M. Synthesis, X-ray crystal structures and thermal analyses of some new antimicrobial zinc complexes: New configurations and nano-size structures. *Mater. Sci. Eng. C* **2016**, 61, 809-823.
46. Basu, U.; Pant, I.; Hussain, A.; Kondaiah, P.; Chakravarty, A.R. Iron(III) complexes of a pyridoxal Schiff base for enhanced cellular uptake with selectivity and remarkable photocytotoxicity. *Inorg. Chem.* **2015**, 54, 3748-3758.
47. Hazra, M.; Dolai, T.; Pandey, A.; Dey, S.K.; Patra, A. Synthesis and characterisation of copper(II) complexes with tridentate NNO functionalized ligand: Density function theory study, DNA binding mechanism, optical properties, and biological application. *Bioinorg. Chem. Appl.* **2014**, 2014, Article ID 104046, 13 pages.